

# 15-kV Single-Bias All-Optical ETO Thyristor

A. Mojab and S.K. Mazumder

Laboratory for Energy and Switching-Electronics Systems  
University of Illinois at Chicago (UIC)  
851 South Morgan Street, Chicago, IL: 60607  
Emails: {mazumder, amojab2}@uic.edu

L. Cheng<sup>1</sup>, A.K. Agarwal<sup>2</sup>, and C.J. Scozzie<sup>3</sup>

<sup>1</sup>Cree Inc., 4600 Silicon Dr., Durham, NC 27703, USA  
<sup>2</sup>U.S. Department of Energy, 1000 Independence Ave. SW,  
Washington DC 20585, USA  
<sup>3</sup>U.S. Army Research Laboratory, 2800 Powder Mill Rd,  
Adelphi, MD, USA

**Abstract**— A new all-optical emitter-turn-off (ETO) configuration is proposed in this paper which is operated under 15 kV single bias and a current of 10 A. This ETO is completely controlled by two optical signals, one for the 15 kV SiC gate-turn-off (GTO) thyristor and the other one for a triggering low-voltage optically controlled Si switch. The latter, called optically-triggered power transistor (OTPT), is used in series with the anode contact of the SiC GTO thyristor in order to handle the current switching between anode and gate path of the SiC GTO thyristor. This OTPT is triggered with a 5-W laser of 808-nm wavelength and the main SiC GTO thyristor is triggered with a laser having a low wavelength of 266 nm. The voltage drop on the OTPT during the on-state is controlled by the power of the laser. For an optical power of 5 W, the structure is optimized to have an on-state voltage of 0.2 V at the junction temperature of 200 °C. This is less than 0.002% of the total bias of 15 kV.

## I. INTRODUCTION

The impact of controllable high-voltage (HV) power semiconductor devices on multiple high-power applications is expected to be profound [1]-[4]. With the rapid growth of wide-bandgap materials and device technologies, the goal of realizing controllable HV devices is slowly materializing. HV SiC DMOSFETs, SiC IGBTs, SiC GTOs have been demonstrated [5]-[8]. However, they all require plurality of biases for activation. In this paper, an optical ETO [9] is outlined that operates with only the power bias as compared to monolithic and hybrid electrical ETOs [10], [11] as well as other bipolar and insulated-gate device mentioned above. This is achieved via optical switching and self-triggering mechanisms as narrated in the subsequent section. Further, the simple optical switching scheme holds promise for seamless operation of series of the device for even higher voltage operation since necessity for complex floating ground gate drivers for electrical HV devices are eliminated [12], [13].

## II. PRINCIPLE OF OPERATION OF OPTICALLY-TRIGGERED ETO

### A. Optically-Triggered ETO

In Fig. 1, the schematic diagram of this electrically-triggered ETO [11] along with the newly-proposed optically-triggered ETO [9] is shown. The PMOS transistor in electrically-triggered ETO is now substituted with the OTPT in optically-triggered ETO. Furthermore, the SiC GTO thyristor in the

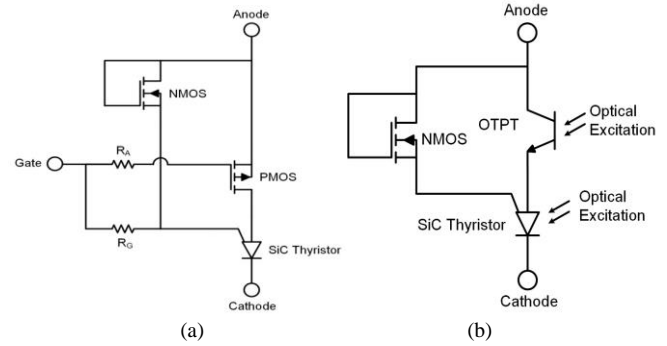


Fig. 1: Schematic diagram of the (a) conventional electrically-triggered ETO based on electrical SiC GTO thyristor [11] and (b) proposed single-bias all optically-triggered ETO based on optical SiC GTO thyristor (with optical window in the gate region that is excited during turn-on and an electrical gate that supports turn-off current) and a triggering OTPT.

optically-triggered ETO is also capable of being latched with a laser beam through a pilot thyristor. For more information about the structure and operation of the SiC GTO thyristor, see [14]. The switching operations for both structures are similar except that the electrical control signal in previous electrically-triggered ETO is now replaced with two optical control signals. In the on-state condition, the Si PMOS transistor in the electrically-triggered ETO or the OTPT in the optically-triggered ETO is turned on. The gate terminal in the electrically-triggered ETO is biased with a negative voltage of -15 V. This negative voltage will turn on the main SiC GTO thyristor as well. In the optically-triggered ETO, the OTPT is illuminated with an 808-nm laser beam and the SiC GTO thyristor is triggered with a 266-nm laser. Once the thyristor is latched, the beam can be removed, but illumination on the OTPT should be kept until the end of the on-state cycle.

In the off-state, the PMOS transistor in the electrically-triggered ETO or the OTPT in the optically-triggered ETO is turned off. A zero gate bias of the electrically-triggered ETO turns off the PMOS transistor. While both the PMOS and the OTPT are off, the voltage across them is increased and this will cause the self-gated NMOS transistor to turn on automatically. The anode current of the SiC GTO thyristor is then diverted to the gate path. The positive current flowing into the gate contact of the SiC GTO thyristor will force it to turn off rapidly under unity-gain turn-off condition.

This work is supported in part by U.S. NSF (award no. 1202384) and U.S. ARPA-E (award no. DE-AR0000336). However, any opinions, findings, conclusions, or recommendations expressed herein are those of the authors and do not necessarily reflect the views of the NSF or ARPA-E. At Cree Inc., this work was supported by C. Scozzie of the US Army Research Laboratory in Adelphi, MD.

### B. 15-kV SiC GTO Thyristor

Details of the basic 15-kV SiC GTO thyristor (Fig. 2) used in the optically-triggered ETO are provided in [14]. Currently, a thickness of more than 120  $\mu\text{m}$  is achieved for the p-type epitaxial drift layer and the drift-layer doping concentration has been reduced to less than  $2 \times 10^{14} \text{ cm}^{-3}$ . A bevel structure [14] is used to further increase the breakdown voltage of the SiC GTO thyristor. With these improvements, a breakdown voltage of more than 15 kV is achieved with extremely low leakage current in the SiC GTO thyristor.

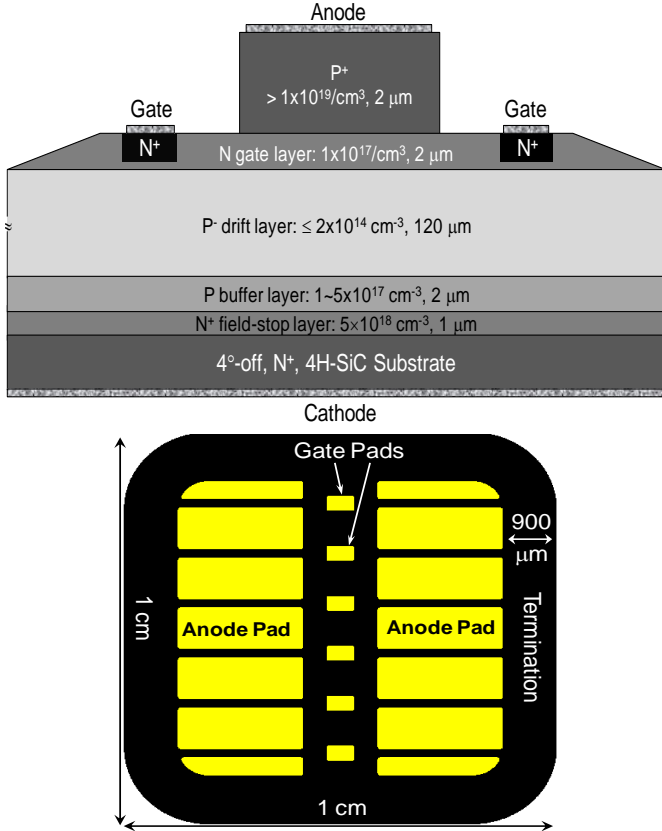


Fig. 2: Schematic cross-section and layout of the 15-kV SiC GTO thyristor.

To trigger the main SiC GTO thyristor, an integrated pilot thyristor having same epitaxial structure as the main thyristor is used in parallel with the emitter electrically shorted to the gate of the main SiC GTO thyristor. The photo-generated current is then pushed into the main gate terminal of the SiC GTO thyristor, which can trigger the SiC GTO thyristor to the latched condition. This approach is illustrated in Fig. 3 [15].

### C. Optically-Triggered Power Transistor (OTPT)

The schematic cross-section of the OTPT is shown in Fig. 4. The on-resistance of this optical switch is controlled by using different optical wavelengths and power intensities. The driving laser in our work has a wavelength of 808 nm and an optical power up to 7 W. At 5 W of optical power, the OTPT on-state voltage is reduced to less than 0.2 V.

When the OTPT is in the dark situation, the p-type base layer is acting as the blocking layer and only a low leakage current is passing through the OTPT. When the OTPT is illuminated, hole-electron pairs are generated in that p-base

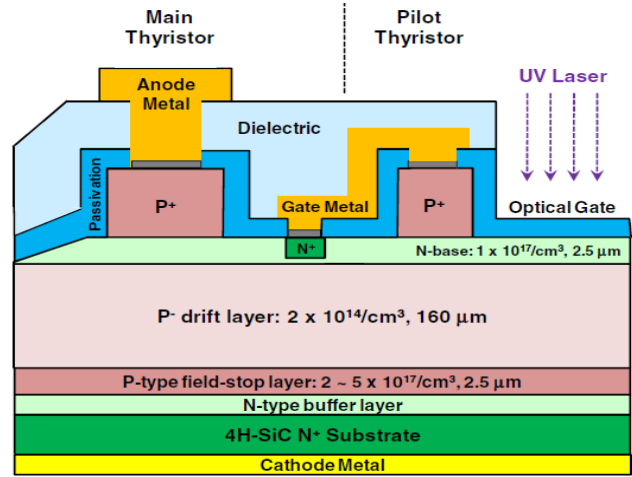


Fig. 3: Illustration of an integrated optical SiC thyristor comprising a pilot thyristor. This mechanism is used to trigger the optical thyristor in Fig. 1b.

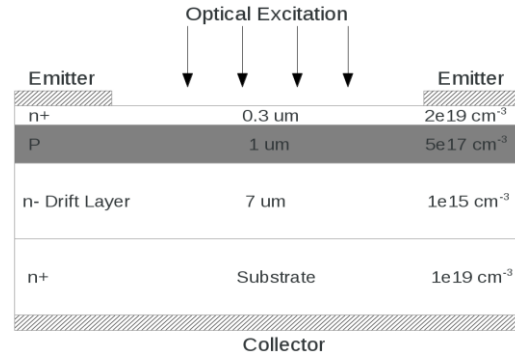


Fig. 4: Device structure for the OTPT.

layer and now this layer is conducting electrons moving from emitter to the collector terminal. The conductivity of the p-type base layer is dependent of the optical intensity of the laser beam. The higher illumination intensity will yield high carrier conductivity and reduced on-state voltage.

The thick N-drift layer is responsible for blocking high voltage. This high overshoot voltage usually occurs when the optical ETO is in transition from the on- to the off-state. A thickness of about 7  $\mu\text{m}$  and a doping of  $10^{15} \text{ cm}^{-3}$  is enough to block a voltage of more than 70 V. However our simulations show that OTPT breakdown voltage is also a function of the p-base doping level. The p-base layer is first optimized to obtain the required on-state voltage and fall time.

### III. RESULTS AND DISCUSSION

The optically triggered ETO structure is simulated using Silvaco modules. For device-level simulations, Athena and Devedit modules are used to fabricate the OTPT and GTO thyristor devices. Then, the fabricated structures are inserted in Atlas module with mixed-mode, device and circuit simulations. A set of important and necessary physical models have been used in our Silvaco device-level simulations, such as concentration dependent mobility, lateral electric field-dependent mobility, Shockley-Read-Hall recombination and Auger recombination. For impact-ionization modeling, Selberherr model is used for the silicon-based OTPT and anisotropic model is used for the SiC-based GTO thyristor.

The lifetime is properly set for each of the layers of the SiC-based GTO thyristor. To have a high breakdown voltage of more than 15 kV, the drift layer in the SiC GTO thyristor has a thickness of 120  $\mu\text{m}$  and a doping of  $2 \times 10^{14} \text{ cm}^{-3}$ . Furthermore, to have a high conductivity during the ETO on-state, the drift layer lifetime should be high enough. A lifetime of 1  $\mu\text{s}$  is considered for the thick drift layer of the GTO thyristor.

#### A. SiC GTO: Effect of Drift-Layer Carrier Lifetime

Decreasing the defect in the epitaxial layer during its growth is an important factor in improving the performance of the SiC GTO thyristor. Higher carrier lifetime leads to better thick drift layer conductivity (lower voltage drop) during the thyristor on-state (Fig. 5). The drawback of having longer lifetime is the high delay in the device turn-off; however, this can be compensated by using higher thyristor driving currents. Cree Inc. announced that they have achieved the ability to attain a drift-layer carrier lifetime between 2 and 5  $\mu\text{s}$ . The advantage of having higher lifetime is the fast SiC GTO thyristor firing and low conduction voltage drop, which are big challenges in high-power electronic devices.

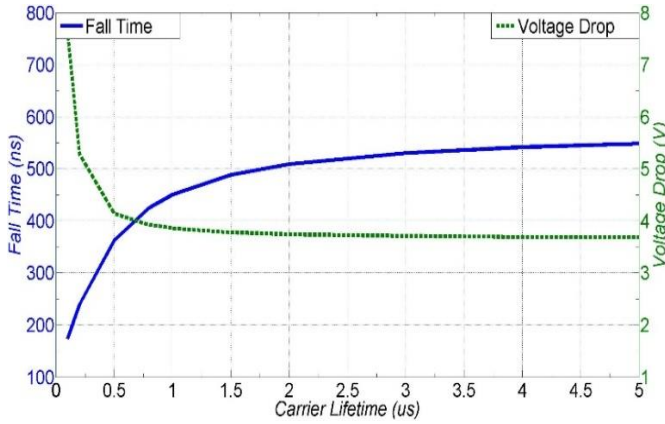


Fig. 5. Fall time and voltage drop vs. carrier lifetime for the optically-triggered ETO thyristor.

#### B. Steady-State and Transient Response of the OTPT

The voltage drop across the OTPT during the transient turn-off of the ETO increases rapidly and forms a fast and high overshoot voltage which is related to the parasitic inductances in the gate and anode path of the main SiC GTO thyristor. Based on our simulations, an overshoot voltage of about 50 V is seen when the parasitic inductances is 100 nH for the worst case condition. To make sure that our OTPT is operating properly during the overshoots, the breakdown voltage should be more than 50 V. Our initial designed goal was to achieve a breakdown voltage of about 70 V. Therefore, we used a thick drift layer of 7  $\mu\text{m}$  with a doping level of  $10^{15} \text{ cm}^{-3}$  for the OTPT device. In Figs. 6a and 6b, the simulation and experimental results for the OTPT breakdown is shown. As expected, a good agreement is observed.

Fig. 7 shows the transient response of the OTPT operating in standalone mode. The dashed curve represents the optical pulse exciting the OTPT while the solid curve shows the current through the OTPT. A bias voltage of 50 V is applied

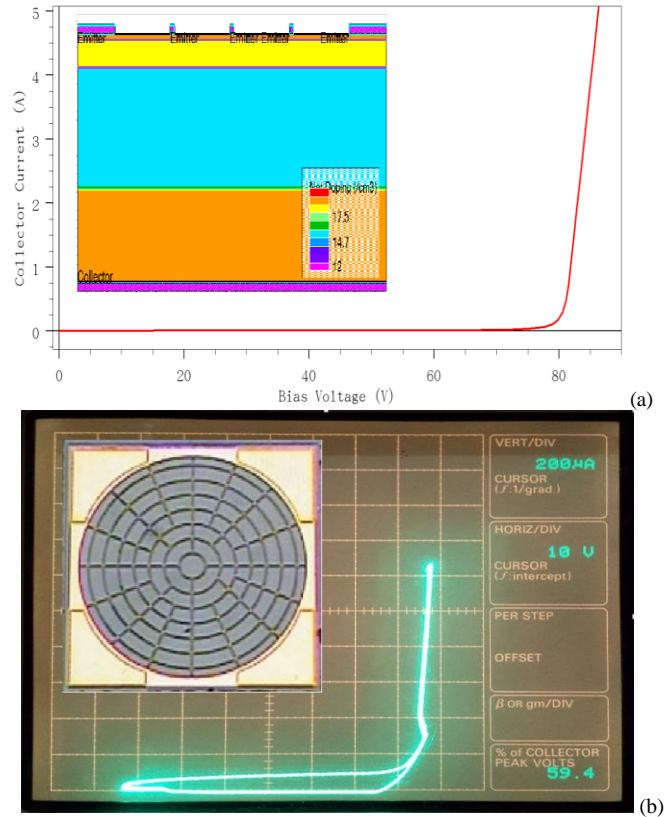


Fig. 6: OTPT breakdown voltage measured using (a) Silvaco based simulation and (b) curve-tracer based result on the experimental OTPT.

with a load current of 10 A. The optical control signal is a laser pulse of 808-nm wavelength with an optical intensity of 5 W. The frequency of the optical pulse is 20 kHz with a duty cycle of 40%. Simulation results show a rise and fall times of 18 ns and 102 ns, respectively, and the delay in fall time is 222 ns. The voltage drop across the OTPT is 0.16 V during the on-state which shows a small on-resistance of 16 m $\Omega$  under 5 W of optical illumination. The on-resistance of the OTPT can be decreased further by increasing the optical intensity.

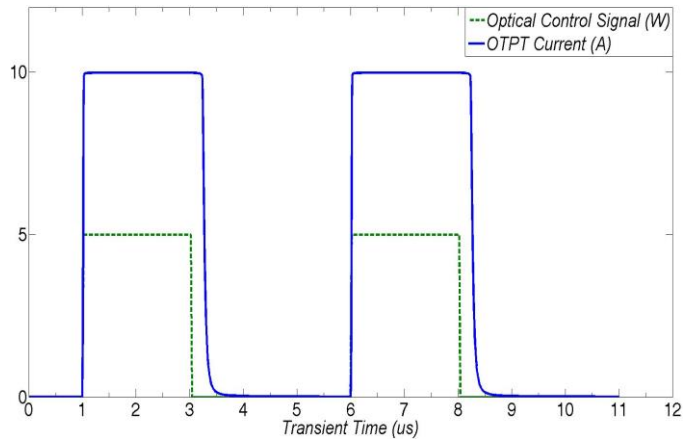


Fig. 7: Transient response for the OTPT current.

#### C. Transient Response of the Optical ETO

The switching behavior of the optically-triggered ETO is investigated next. In Fig. 8a, the voltage across the load and

the optical control signal on the OTPT is shown. The optical signals triggering the OTPT and the optical SiC GTO thyristor are simultaneously activated. However, they have different wavelengths and optical intensities. The laser beam activating the optical SiC GTO thyristor has a wavelength of 266 nm and needs limited optical power while the laser beam exciting the OTPT has a wavelength of 808 nm and a power of 5 W. During the on state, the voltage across the thyristor and across the OTPT is 4.1 V and 0.2 V, respectively, leading to a total on-state voltage drop of 4.3 V. This is less than 0.03% of the total bias voltage of 15 kV.

During the turn off of the optical ETO thyristor, the maximum transient voltage on the OTPT is about 6 V (parasitic inductances are assumed to be zero). Fig. 8b shows the results for the thyristor currents versus transient time for the optical ETO. Rise and fall times of the ETO cathode current (or load current) is found to be 27 ns and 310 ns respectively. As shown in Fig. 8, a smooth commutation current from anode to gate is observed. The turn-off delay is the combination of the fall time of the anode current and the period that the gate is conducting. This turn-off delay is found to be about 800 ns.

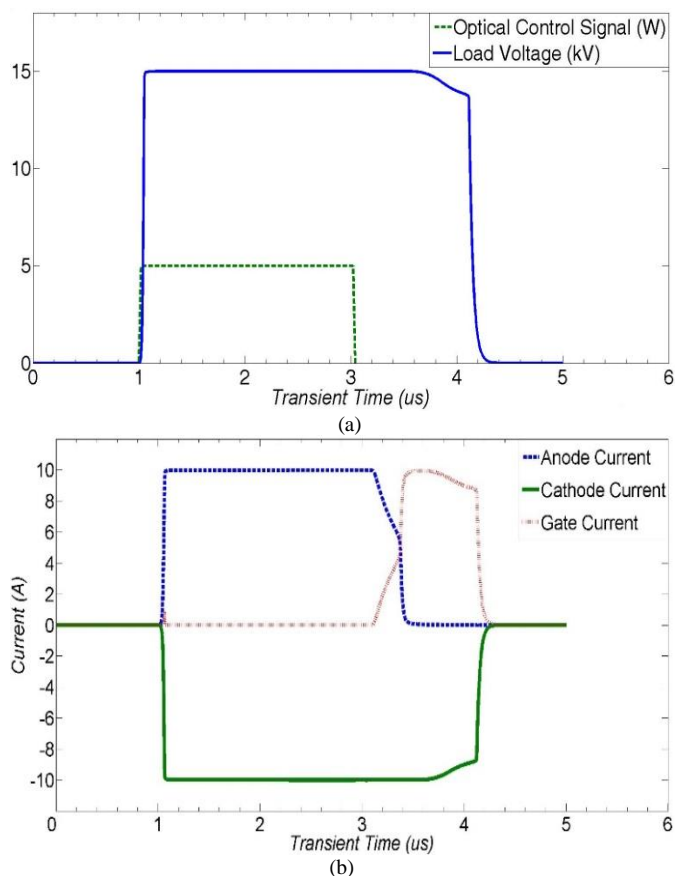


Fig. 8: (a) Voltage across the load and the optical control signal on the OTPT. (b) Output currents for the optical ETO thyristor.

#### IV. CONCLUSION

In this paper, an optical ETO thyristor, comprising an optically switched 15-kV SiC GTO thyristor and a triggering low-voltage ( $\leq 70$  V) OTPT, is described along with structural details, principles of operation, and results. The results of the all-optical single-bias ETO demonstrate the feasibility of the device and high-voltage and high-frequency of operation.

#### REFERENCES

- [1] B.J. Baliga, Fundamentals of power semiconductor devices, Springer, 2008.
- [2] A. Agarwal, Q. Zhang, A. Burk, R. Callanan, and S.K. Mazumder, "Prospects of bipolar power devices in silicon carbide", Invited Paper, IEEE Industrial Electronics Conference, pp. 2879-2884, 2008.
- [3] Q. Zhang, R. Callanan, M.K. Das, S.H. Ryu, A.K. Agarwal, and J.W. Palmour, "SiC power devices for microgrids," IEEE Transactions on Power Elec., vol. 25, no. 12, pp. 289-2896, 2010.
- [4] T.P. Chow, "Progress in high voltage SiC and GaN power switching devices," Materials Science Forum, vols. 778-780, pp. 1077-1082, 2014.
- [5] S. Ryu, S. Krishnaswami, B. Hull, J. Richmond, A. Agarwal, and A. Hefner, "10 kV, 5A 4H-SiC power DMOSFET", in Proceedings of the 18<sup>th</sup> International Symposium on Power Semiconductor Devices and IC's, Naples, Italy, June 4-8, 2006.
- [6] M. Das, Q. Zhang, R. Callanan, C. Capell, J. Claytoun, M. Donfrio, S. Haney, F. Husna, C. Jonas, J. Richmond, J. J. Sumakeris. "A 13 kV 4H-SiC N-channel IGBT with low  $R_{diff,on}$  and fast switching," Materials Science Forum, vols. 600-603, 2009, pp. 1183-1186.
- [7] Y.Sui, X. Wang, and J.A. Cooper, "High voltage self-aligned pchannel DMOS-IGBTs in 4H-SiC," IEEE Electron Device Lett., 28, 728-730, 2007.
- [8] A.K. Agarwal, B. Damsky, J. Richmond, S. Krishnaswami, C. Capell, S.-H. Ryu, and J.W. Palmour, "The first demonstration of the 1 cm x 1 cm SiC Thyristor chip", International Symposium on Power Semiconductor Devices & IC's, May 23-26, 2005.
- [9] S.K. Mazumder, "Photonically activated single bias fast switching integrated thyristor," U.S. Patent Application# 13281207, filed in 2011.
- [10] M.S. Shekar, B.J. Baliga, M. Nandakumar, S. Tandon, and A. Reisman, "Characteristics of the emitter-switched thyristor," IEEE Transactions on Electron Devices, vol. 38, no. 7, pp. 1619-1623, 1991.
- [11] J. Wang and A. Huang, "Design and characterization of high-voltage silicon carbide emitter turn-off thyristor," IEEE Transactions on Power Electronics, vol. 24, Issue 5, pp. 1189-1197, May 2009.
- [12] S.K. Mazumder and T. Sarkar, "Optically-triggered power system and devices," USPTO Patent# 8,294,078, awarded on October 23, 2012.
- [13] S.K. Mazumder and T. Sarkar, "Optically-activated gate control for power electronics," IEEE Transactions on Power Electronics, vol. 26, no. 10, pp. 2863-2886, 2011.
- [14] L. Cheng, A.K. Agarwal, C. Capell, M. O'Loughlin, K. Lam, J. Richmond, A. Burk, J. Palmour, A.A. Ogunniyi, H.K. O'Brien, and C. J. Scozzie, "15 kV, large Area (1 cm<sup>2</sup>) 4H-SiC p-type gate turn-off thyristors," Proceedings of the 9<sup>th</sup> European Conference on Silicon Carbide and Related Materials (ECSCRM'12), Mat. Sci. Forum, Vols. 740-742 (2013), pp. 978-981, Saint Petersburg, Russia, Sept. 2-6, 2012.
- [15] S.L. Rumyantsev, M.E. Levenshtein, M.S. Shur, L. Cheng, A.K. Agarwal, and J.W. Palmour, "Optical triggering of high-voltage 18-kV-class 4H-SiC thyristors," Semiconductor Science Technology, doi:10.1088/0268-1242/28/12/125017, vo. 28, pp. 1-4, 2013.